Autofluorescence Maps of Atherosclerotic Human Arteries—A New Technique in Medical Imaging

MICHELE SARTORI, ROLAND SAUERBREY, MEMBER, IEEE, SHOICHI KUBODERA, FRANK K. TITTEL, FELLOW, IEEE, ROBERT ROBERTS, AND PHILIP D. HENRY

Abstract—**A new medical imaging technique for arterial walls based on laser-induced autofluorescence spectroscopy is reported. The internal surface of isolated arteries with or without atherosclerosis is irradiated with an argon ion laser (458 nm) and the peak intensity of the excited autofluorescence spectrum is related to the composition of the arterial wall. The higher autofluorescence intensity in the range between approximately 480 and 630 nm for grossly calcified tissue compared to normal or noncalcified atherosclerotic tissue is used to produce maps of the arterial wall. These images delineate the calcified areas of the sample with good spatial resolution. If this technique can be adapted to the endoscopic visualization of arteries *in vivo* (angioscopy), it could become an important tool for the diagnosis of atherosclerosis and for the monitoring of atheroma ablation during laser angioplasty.**

I. Introduction

THE possible use of low-energy lasers for the diagnostic characterization of arterial wall structure was recently proposed [1]–[7]. Blue laser radiation was used to excite autofluorescence of human arteries in the green to the orange portion of the visible spectrum. In previous studies attempts were made to distinguish normal from atherosclerotic artery segments on the basis of the shapes of the regional autofluorescence spectra. It is shown in this paper that the *intensity* of the autofluorescence regardless of its spectral shape can be used to distinguish grossly calcified regions from normal or noncalcific atherosclerotic regions of isolated arteries. The spectral data were used to construct fluorescence intensity images that delineate grossly calcified areas of the arterial wall. If such images could be obtained *in vivo* by angioscopic techniques, fluoresence mapping might prove useful for the localization of atherosclerotic lesions and selective laser ablation.

II. Experimental Setup and Procedure

The experimental setup is shown in Fig. 1. An argon ion laser was tuned to the 457.9 nm transition. The laser radiation was coupled into an optical fiber and delivered to the tissue sample. The fluorescence radiation emitted from the tissue surface was guided by a second optical fiber to a 0.25 m spectrometer equipped with an OMA III detector system. The spectral resolution of the optical setup was about 0.5 nm. A filter with a cutoff wavelength of 470 nm (10 percent transmission) was employed in front of the spectrometer in order to suppress the strong signal at 458 nm due to back-reflected laser light from the tissue. The OMA III was connected to an IBM minicomputer for data handling. The autofluorescence spectra were stored on disk for further processing in the imaging system.

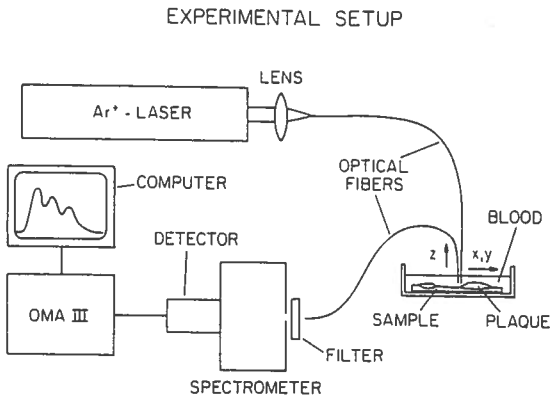

Fig. 1. Experimental setup. An argon ion laser operated at 458 nm is coupled in an optical fiber with 600 μm core diameter. It excites autofluorescence in the tissue surface, which is guided by a second fiber to the entrance slit of a 0.25 m spectrometer. The spectra are registered by an OMA III, and stored and displayed by a computer.

Six artery samples were excised from the aorta of fresh (less than 12 h old) human cadavers. The presence or absence of atherosclerotic lesions was determined by careful inspection and microscopic evaluation of frozen tissue stained for lipids with oil red O. No X-rays for detecting the calcified regions were taken.

For the detection of autofluorescence spectra, the fiber for delivery of the 458 nm Ar^+ laser light and the fiber for the fluorescence collection leading to the spectrometer were mounted parallel and as close as possible to each other in a fixed fiber holder. The core fiber diameter was 600 μm and all fiber ends were polished. The tissue samples were pinned to a piece of cardboard which was mounted to a translational stage that could be moved in x, y, and z directions by means of micrometer screws.

Manuscript received February 20, 1987; revised June 9, 1987. This work was supported by the National Institutes of Health under Contracts 1 RO1 HL 36894-01 and F 32-HL 0730801.

M. Sartori, R. Roberts, and P. D. Henry are with the Section of Cardiology, Baylor College of Medicine, Houston, TX 77030.

R. Sauerbrey, S. Kubodera, and F. K. Tittel are with the Department of Electrical and Computer Engineering and the Quantum Institute, Rice University, Houston, TX 77251.

IEEE Log Number 8716270.

Rulers were glued at the sides of the tissue samples to identify the position of the irradiated area. For detection of the autofluorescence, the distance in z direction between the two fiber tips and the tissue surface was kept as constant as possible when the tissue was moved in the xy plane (Fig. 1). In this study the angle between the tissue surface and the fiber was approximately 90°. Since the fluorescence originates from the volume of the tissue, it is emitted isotropically. Therefore, this technique should work as well under angles of incidence different from 90°, although this was not attempted in the present experiments.

Autofluorescence spectra from different regions of a typical sample are shown in Fig. 2. Fig. 2(a) illustrates a region that was free of atherosclerotic changes on macroscopic and microscopic examination. Three distinct peaks at 520, 555, and 595 nm are clearly visible. Fig. 2(b) shows a region containing gross calcifications. The spectrum exhibits a characteristic change in qualitative agreement with previous results [2]–[7]. The middle peak at 555 nm increases in height leading to a fusion of the peaks at 520 and 555 nm. In earlier reports it was suggested to utilize this characteristic change in the spectral shape of the autofluorescence for the detection of atherosclerotic lesions.

However, even more striking than the change in spectral shape between Fig. 2(a) and (b) is the difference in autofluorescence intensity. The excitation intensity at 458 nm was 400 μWcm^{-2} for both spectra, and the distance of the fiber tip from the tissue was the same in both cases. Nevertheless, the autofluorescence intensity for the calcific region was more than four times that of the noncalcific region.

This large and easily detectable difference between normal and calcified sections of the aorta was used in order to produce a fluorescence intensity image of the arterial wall. The samples were divided in squares of 2.5 × 2.5 mm and the coordinates of the irradiated spots in the xy plane were determined (Figs. 3(a) and 4(a)). The autofluorescence spectrum of each square was detected and stored on disk. Then, the peak intensity in each spectrum at 520 nm and its xy coordinates were fed into a digital image processor (PSICOM 327). The difference between maximum and minimum peak intensities recorded in the xy plane was divided in 128 equal intervals and a color was assigned to each interval, with red corresponding to the highest and blue to the lowest peak intensity. The colors change according to the spectrum in order to indicate intermediate intensity values, i.e., intermediate intensity values are represented by intermediate colors. In order to generate a smooth transition in color between adjacent squares, two-dimensional cubic spline interpolation was used. In this way peak intensity maps of the arterial samples could be produced.

III. Results and Discussion

Peak intensity fluorescence maps of two representative samples are shown in Figs. 3(b) and 4(b). They may be compared to photographs of these samples shown in Figs. 3(a) and 4(a). The fluorescence map of sample number 4 shown in Fig. 3(a) was taken between $x_1 = 20$ mm and $x_2 = 40$ mm, and between $y_1 = 2.5$ mm and $y_2 = 25$ mm, i.e., only the central portion of the photograph given in Fig. 3(a) is shown in Fig. 3(b). The fluorescence map of sample number 5 shown in Fig. 4(b) covers almost the whole photograph [Fig. 4(a)] except for the edges. It was taken between $x_1 = 2.5$ mm and $x_2 = 30$ mm, and between $y_1 = 2.5$ mm and $y_2 = 27.5$ mm. Sample number 4 exhibits a grossly calcified area close to the center [Fig. 3(a)]. Comparison with the fluorescence map shows that this is exactly reproduced by the red and yellow colors corresponding to the highest fluorescence peak intensities [Fig. 3(b)]. The two areas of lipid-rich tissue to the left-hand side of the calcification are clearly shown by green colors. In sample number 5 gross calcification is detected in a ring-shaped region in the upper part of the photograph as well as on the left-hand side in the middle and close to the lower right-hand side corner [Fig. 4(a)]. All these structures are correctly represented by the red and yellow colors in the fluorescence map [Fig. 4(b)]. Fine details, such as the extension of the calcified ring into the fatty tissue at its lowest point close to the center of the sample,

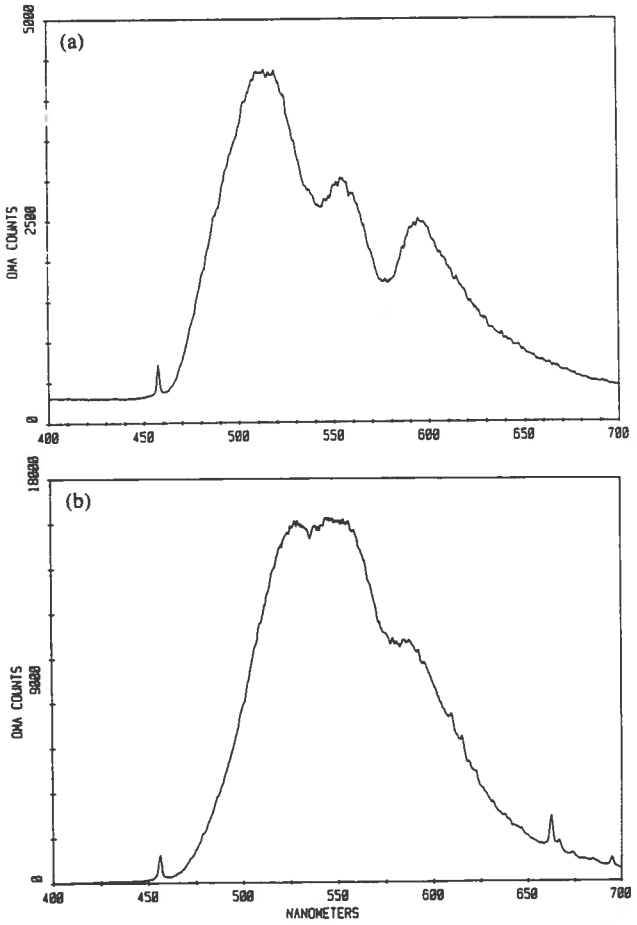

Fig. 2. Autofluorescence spectra from human arteries. (a) Normal section of tissue. It shows the characteristic three peaks. (b) Calcified section of tissue. The spectrum shows almost no structure but is more than four times more intense than the autofluorescence intensity from normal tissue.

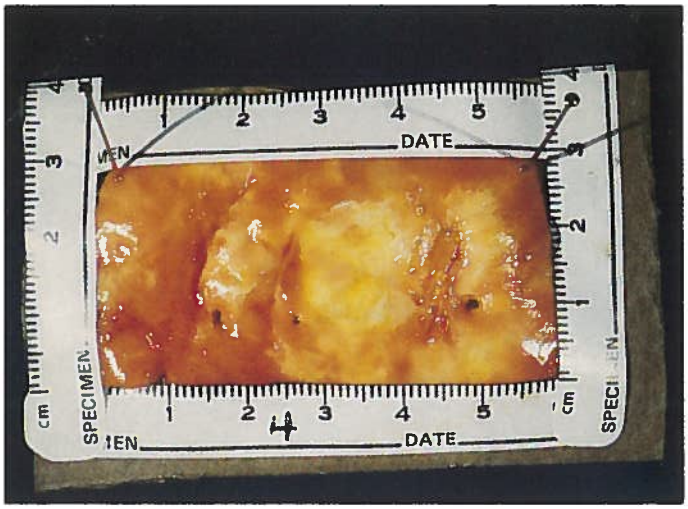

(a)

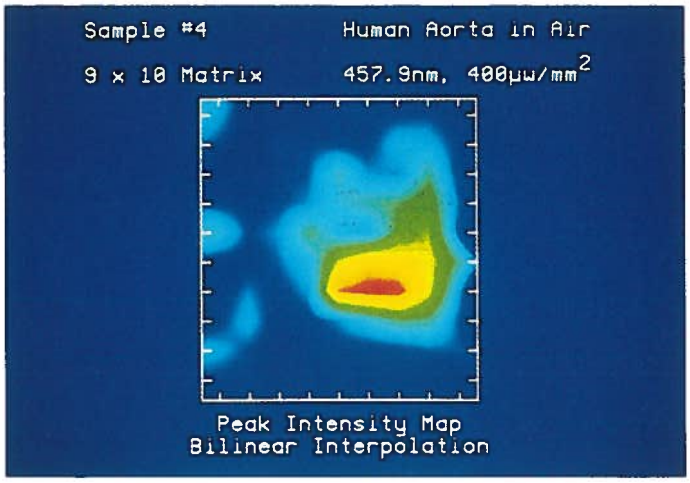

(b)

Fig. 3. (a) Photograph of a section of human artery. A large somewhat structured calcified area is visible in the center. (b) Autofluorescence map of the central portion of (a). The map was taken between the coordinates $x_1 = 20$ mm, $x_2 = 40$ mm, and $y_1 = 2.5$ mm, $y_2 = 25$ mm. The calcified parts appear as red and yellow areas, whereas the normal and fatty tissue is blue and dark green.

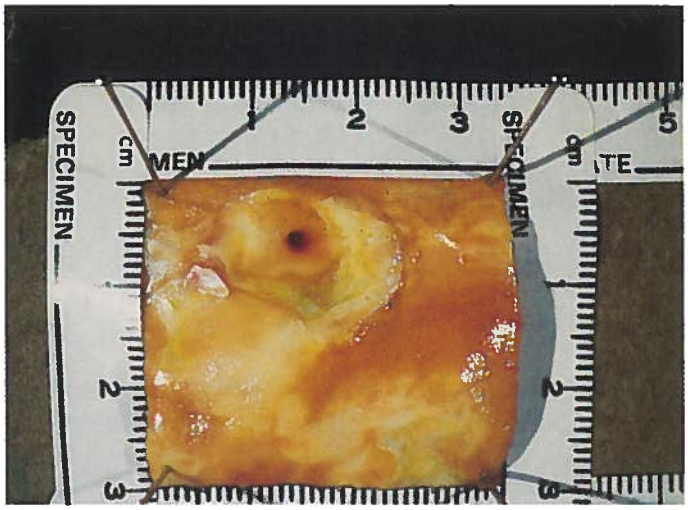

(a)

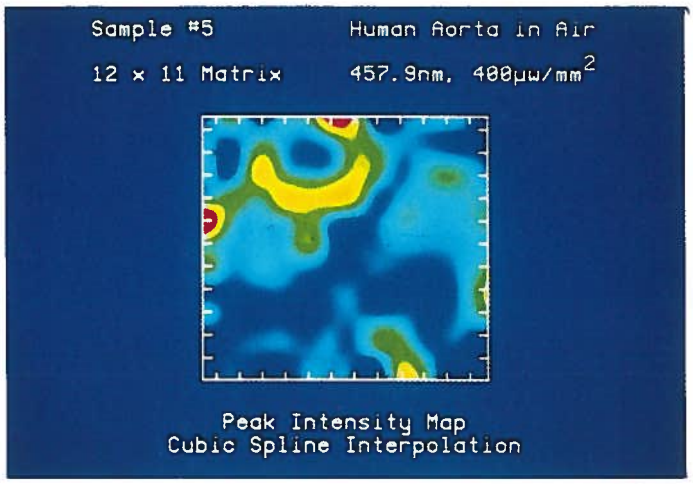

(b)

Fig. 4. (a) Photograph of an atherosclerotic tissue sample exhibiting various highly spatially structured calcified regions. Most notable is a ring-shaped area in the upper half of the sample. (b) Autofluorescence map of (a) between the coordinates $x_1 = 2.5$ mm, $x_2 = 30$ mm, and $y_1 = 2.5$ mm, $y_2 = 27.5$ mm. The red and yellow areas clearly show all the calcified structures. Even fine details, such as the extension of the calcified ring towards the center of the sample, are shown.

are also revealed by the fluorescence map. It is important to note that in both maps (Figs. 3 and 4) no bright colors (yellow, red) appear in portions of the samples where fibrous or fatty tissue dominates. The maps appear to exhibit an exact image of the grossly calcified portions of the tissue.

The spatial resolution of the fluorescence maps is determined by the number of measured spectra per area. In this investigation, it is given by the size of the individual areas of 2.5 × 2.5 mm. It appears likely that the resolution could increase substantially with improved data handling. Ultimately, the spatial resolution should be limited only by the fiber diameter and could reach the 100 to 10 μm range.

The maps shown in Figs. 3 and 4 have been obtained in air. For clinical application of this technique it is important that the large differences in autofluorescence intensity between calcific and noncalcific tissue persist when air is replaced by blood and when the fiber tips are brought in contact with the tissue. A method adapted to the mapping of tissue samples immersed in blood is currently under development in our laboratories.

Since the intensity of the autofluorescence radiation is used to distinguish calcific from noncalcific tissue, the distance between the optical fibers and the tissue sample in z direction (Fig. 1) is critical in these experiments. When either the distance of the fiber carrying the excitation laser or the distance of the fiber for detection of the fluorescence to the tissue sample change in an uncontrolled way, too high or too low autofluorescence inten-

sities may be detected and calcified spots may be missed or artificially created. Therefore, care was taken to keep the fiber-sample distance constant to both fibers. Nevertheless, slight distance variations are unavoidable due to the uneven surface of the tissue sample. Estimates of intensity variation due to this effect show that they should be considerably smaller than the detected and mapped intensity differences between calcific and noncalcific tissue. Also, the internal consistency of the reported data indicates that this effect, although not completely negligible, is not large enough to substantially impair image quality. Although the results presented in Figs. 3 and 4 have been produced with a fiber-artery distance of about 1 mm, most recent investigations show that the fluorescence spectra remain unchanged when both fibers are brought into immediate contact with the tissue surface. This insensitivity of the fluorescence to fiber positioning should facilitate the adaptation of the method to *in vivo* use.

IV. Summary and Conclusions

It is demonstrated in this short paper that images of the calcified regions of arterial samples can be produced based on the observation that the autofluorescence between 480 and 630 nm is considerably more intense for calcified tissue than for noncalcified tissue. The quality of the images is good and allows for a unique identification of calcified areas in the tissue.

The clinical applications of this technique appear very promising. Low intensity visible laser radiation may be transmitted through an optical fiber advanced through an intra-arterial catheter. Detection of the autofluorescence peak intensity as a function of the position of the fiber tip would yield complete images of the inner arterial wall for diagnostic purposes. The development of a laser angioplasty system permitting alternative fluorescence imaging and ablation should improve the safety of laser angioplasty.

References

[1] C. Kitrell, R. L. Willet, C. de las Santos-Pacheo, N. B. Ratliff, J. R. Kramer, E. G. Malk, and M. S. Feld, "Diagnosis of fibrous arterial atherosclerosis using fluorescence," *Appl. Opt.*, vol. 24, pp. 2280–2281, 1985.

[2] M. S. Feld, C. Kitrell, R. E. Cothran, and B. I. Sacks, "Laser angiosurgery with spectral diagnostics," in *Proc. CLEO'86*, San Francisco, CA, June 9–13, 1986.

[3] R. Richards-Kertum, C. Kitrell, and M. S. Feld, "Laser-induced spectral diagnosis of atherosclerosis," in *Proc. CLEO'86*, San Francisco, CA, June 9–13, 1986.

[4] M. P. Sartori, P. D. Henry, R. Roberts, R. C. Chin, and M. J. Berry, "Estimation of arterial wall thickness and detection of atherosclerosis by laser induced argon fluorescence," *J. Amer. Coll. Cardiol.*, vol. 7, p. 76A, 1986.

[5] M. P. Sartori, C. Bossaller, D. Weilbacher, P. D. Henry, R. Roberts, R. C. Chin, G. L. Valderrama, and M. J. Berry, "Detection of atherosclerotic plaques and characterization of arterial wall structure by laser-induced fluorescence," *Circulation*, vol. 74, no. II, p. 25, 1986.

[6] L. I. Deckelbaum, M. L. Stetz, J. K. Lam, K. S. Clubb, F. Cutruccola, H. S. Cabin, and M. V. Long, "Fiberoptic laser induced fluorescence detection of atherosclerosis and plaque ablation: potential for laser angioplasty guidance," *Circulation*, vol. 74, no. II, p. 27, 1986.

[7] M. P. Sartori, P. D. Henry, R. Roberts, S. Kubodera, R. Sauerbrey, G. L. Valderrama, M. J. Berry, and F. K. Tittel, "Real-time collection of autofluorescence of coronary arteries," in *Proc. 7th Annu. Meet. Amer. Soc. Laser Med. Surg.*, San Francisco, CA, Apr. 11–13, 1987.

Michele Sartori, photograph and biography not available at the time of publication.

Roland Sauerbrey (M'85), for a photograph and biography, see p. 260 of the February 1987 issue of this JOURNAL.

Shoichi Kubodera was born in Tokyo, Japan, on January 8, 1963. He received the B.S. degree in electrical engineering from Keio University, Yokohama, Japan, in 1985.

Since 1986 he has been a graduate student at Rice University, Houston, TX. He has been engaged in research on rare gas halide excimer lasers and their applications in medicine, and in particular, applications in cardiology.

Frank K. Tittel (SM'72–F'86), for a photograph and biography, see p. 261 of the February 1987 issue of this JOURNAL.

Robert Roberts, photograph and biography not available at the time of publication.

Philip D. Henry, photograph and biography not available at the time of publication.